# 2-D Scattering Integral Field Equation Solution Through an IMLS Meshless-Based Approach

Williams Lara Nicomedes, Renato Cardoso Mesquita, and Fernando José da Silva Moreira

Department of Electronics Engineering, Federal University of Minas Gerais, Belo Horizonte, MG Brazil

**In this work, we apply a meshless-based method to a set of integral equations arising in electromagnetic wave propagation and scattering. The objective is not only to solve these equations through a meshless-based method, but also to find a way to build shape functions that could work for any cross-sectional geometry. We have found that the Moving Least Squares (MLS) approximation is not able to provide useful shape functions in every situation. This technique relies on matrix inversions and, according to the geometry, singular matrices can occur. In order to avoid this problem, we have taken the Improved Moving Least Squares (IMLS) approximation, that does not depend upon matrix inversions and then applied it to a number of cross-sectional geometries.**

***Index Terms*—Integral equation, meshless, MLS, scattering.**

## I. Introduction

MESHLESS methods have successfully been applied in mechanics as an alternative to the traditional finite element method (FEM). The Element Free Galerkin method, which is based on the meshless discretization of the weak form, was applied to high-frequency problems in [1]. In this work we take a different approach by applying a meshless discretization directly into the classical integral field equations. We have already solved the problem for a circular cylinder using the MLS approximation [2], but the solution is not as general as to be applied to every cross section form. For other geometries (e.g., rectangular) the MLS approximation fails in providing accurate results, because singular local matrices are obtained, leading to an inconsistent outcome. In this paper we try a different approach through the use of an Improved Moving Least Squares (IMLS) approximation that despite the fact of having to build an orthogonal basis first, it generates diagonal local matrices. Then, there is no need for inversions and the shape functions can be built regardless of the cross-sectional geometry.

## II. Problem Description

In this work, a monochromatic incident plane wave is scattered by a perfect electric conductor (PEC) cylinder infinite in the z-direction. For a $\mathrm{TM^z}$ polarized incident wave, the electric surface current density $\overrightarrow{J_s}$ is directed along the z-direction. One of the equations governing the phenomenon is the electric field integral equation (EFIE) [2]

$$E_z^i(\vec{x}) = \frac{\omega\mu}{4}\oint J_s(\vec{x}')H_0^{(2)}(kR)dl' \tag{1}$$

$E_z^i(\vec{x})$ is the incident electric field at $\vec{x}$, $R = \|\vec{R}\| = \|\vec{x}-\vec{x}'\|$, $\vec{x}$ and $\vec{x}'$ locate the observation and source points at the perimeter, respectively, $\omega = 2\pi f$, where $f$ is the wave frequency, and $H_0^{(2)}$ is the zero-order Hankel function of the second type. The other is the magnetic field integral equation (MFIE) [2]

$$\widehat{n}\times\vec{H}^i(\vec{x}) = J_z(\vec{x})\widehat{z}+\frac{j}{4}\widehat{n}\times\nabla\times\widehat{z}\oint J_z(\vec{x}')H_0^{(2)}(kR)dl' \tag{2}$$

where $\vec{H}^i(\vec{x})$ is the incident magnetic field at $\vec{x}$ and $\widehat{n}$ is the unit surface normal vector. To avoid spurious resonances, one can form the combined field integral equation (CFIE) through a linear combination from the EFIE and MFIE [2]

$$\alpha E_z^i\widehat{z}+(1-\alpha)\eta\widehat{n}\times\vec{H}^i = \frac{\alpha\omega\mu}{4}\oint J_s(\vec{x}')H_0^{(2)}(kR)dl'\widehat{z}$$
$$+(1-\alpha)\eta\left[J_z(\vec{x})\widehat{z}+\frac{j}{4}\widehat{n}\times\nabla\times\widehat{z}\oint J_z(\vec{x}')H_0^{(2)}(kR)dl'\right] \tag{3}$$

where $\alpha$ is a parameter ranging from zero to one and $\eta$ is the intrinsic impedance of the exterior medium.

## III. The Meshless Approach

### A. Overview

The meshless approach begins by spreading nodes over the domain of the problem to be solved. In the present study, the domain of interest is the perimeter of the cylinder cross section. To each node a shape function with compact support is associated. The vicinal region in which the shape function is different from zero is called the *influence domain* of the corresponding node [3]. The main difference between meshless methods and mesh-based methods (like the FEM) is that the *element* concept is not present. The influence domains are arbitrary (the only restriction is that the set of influence domains must cover the entire domain) and can overlap. So, the nodes can be distributed arbitrarily without generating an element mesh.

For a given point (e.g., point $\vec{x} = X$ in Fig. 1), an unknown solution $u$ is expressed as a sum of the contributions of those nodes that exert influence upon $X$, i.e., nodes that extend their influence domains onto $X$ (they are depicted inside the circular shaded region)

$$u(\vec{x}) \sim u^h(\vec{x}) = \sum_{i=1}^{N}\phi_i(\vec{x})\widehat{u}_i = \Phi(\vec{x})u \tag{4}$$

Manuscript received December 23, 2009; accepted March 11, 2010. Current version published July 21, 2010. Corresponding author: W. L. Nicomedes (e-mail: wlnicomedes@yahoo.com.br).

Color versions of one or more of the figures in this paper are available online at http://ieeexplore.ieee.org.

Digital Object Identifier 10.1109/TMAG.2010.2046400

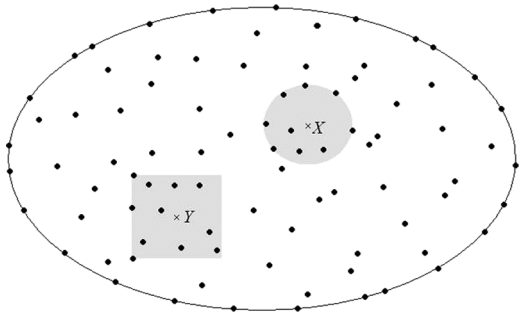


Fig. 1. Nodes spread in a domain. Those ones that influence points X and Y are shown as belonging to regions that surround these points (shaded regions).

### B. Construction of the Shape Functions

*1) The MLS Approximation:* In the MLS, $u^{\boldsymbol{h}}$ is expressed as

$$u^h(\vec{x}) = \sum_{j=1}^{m} p_j(\vec{x}) a_j(\vec{x}) = p^T(\vec{x}) a(\vec{x}) \tag{5}$$

where $\boldsymbol{p}$ is a monomial basis with $m$ terms (e.g., $\boldsymbol{p}(\vec{x}) = [1, x, y]^T$) and $\boldsymbol{a}$ is a vector of coefficients which are functions of $\vec{x}$. We then build a slightly different approximation, by requiring the monomial basis to be calculated at each node

$$u^h(\vec{x}, \vec{x}_i) = \sum_{j=1}^{m} p_j(\vec{x}_i) a_j(\vec{x}) = p^T(\vec{x}_i) a(\vec{x}). \tag{6}$$

The next step is to define a weighted functional $M$

$$M = \sum_{i=1}^{N} w\left(\frac{\|\vec{x} - \vec{x}_i\|}{d_i}\right) \left[u^h(\vec{x}, \vec{x}_i) - \widehat{u}_i\right]^2 \tag{7}$$

or

$$M = \sum_{i=1}^{N} w\left(\frac{\|\vec{x} - \vec{x}_i\|}{d_i}\right) \left[\sum_{j=1}^{m} p_j(\vec{x}_i) a_j(\vec{x}) - \widehat{u}_j\right]^2 \tag{8}$$

$d_i$ is the size of the influence domain associated to node $i$ and $w$ is a function with compact support centered in node $i$. We have chosen it to be a cubic spline [3]

$$w = \begin{cases} \frac{2}{3} - 4r^2 + 4r^3, & 0 \le r \le 0.5 \\ \frac{4}{3} - 4r + 4r^2 - \frac{4}{3}r^3, & 0.5 < r \le 1 \\ 0, & r > 1 \end{cases} \tag{9}$$

where $r = \|\vec{x} - \vec{x}_i\|/d_i$. Looking for the coefficients $a_j$ that minimize the functional, we impose

$$\frac{\partial M}{\partial a} = 0. \tag{10}$$

After some matrix manipulation, we obtain

$$a(\vec{x}) = [A(\vec{x})]^{-1} [B(\vec{x})] u \tag{11}$$

$$u^T = [\widehat{u}_1, \widehat{u}_2, \ldots, \widehat{u}_N] \tag{12}$$

$$A(\vec{x}) = P^T W(\vec{x}) P \tag{13}$$

$$B(\vec{x}) = P^T W(\vec{x}) \tag{14}$$

which are given in terms of

$$P = \begin{bmatrix} p_1(\vec{x}_1) & \cdots & p_m(\vec{x}_1) \\ \vdots & \ddots & \vdots \\ p_1(\vec{x}_N) & \cdots & p_m(\vec{x}_N) \end{bmatrix} \tag{15}$$

$$W(\vec{x}) = \begin{bmatrix} w\left(\frac{\|\vec{x} - \vec{x}_1\|}{d_1}\right) & \cdots & 0 \\ \vdots & \ddots & \vdots \\ 0 & \cdots & w\left(\frac{\|\vec{x} - \vec{x}_N\|}{d_N}\right) \end{bmatrix} \tag{16}$$

By equating the expressions (4) and (5) the shape functions calculated at $\vec{x}$ are readily available

$$\Phi(\vec{x}) = [\phi_1(\vec{x}), \ldots, \phi_N(\vec{x})] = p^T A^{-1}(\vec{x}) B(\vec{x}). \tag{17}$$

The MLS approximation does not always provide useful solutions, because sometimes the $\boldsymbol{A}$ matrices become singular, preventing inversion. This phenomenon occurs for some scatterer geometries, mainly for flat surfaces. To avoid the problem of getting singular matrices a somewhat different approach, known as IMLS was developed and is used in this paper [4].

*2) The IMLS Approximation:* In the IMLS, it is required that the terms of the basis $\boldsymbol{p}$ be orthogonal to each other, *only at the nodal points*. In order to do so, they are viewed as elements of a Hilbert space in which the following inner product between functions $f$ and $g$ is defined

$$\langle f, g \rangle = \sum_{I=1}^{N} w(\vec{x} - \vec{x}_I) f(\vec{x}_I) g(\vec{x}_I) \tag{18}$$

where $w$ is the function defined in (9). The orthogonality condition is assured through the property $(k, j = 1, 2, \ldots, m)$

$$\langle p_k, p_j \rangle = \sum_{I=1}^{N} w(\vec{x} - \vec{x}_I) p_k(\vec{x}_I) p_j(\vec{x}_I) = \begin{cases} A_k, & k = j \\ 0, & k \ne j \end{cases}. \tag{19}$$

As already said, the terms $p_{\mathbf{1}} \cdots p_m$ of the basis $\boldsymbol{p}$ are orthogonal only about the nodal points. Given a general point $\vec{x}$, one finds the $N$ nodes that influence it and evaluates the expression in (19). Bearing in mind the orthogonality at the nodal points, one forms the basis $\boldsymbol{p}$ by requiring its first term to be equal to the unity everywhere, i.e.

$$p_1(\vec{x}) = 1 \tag{20}$$

the next terms are formed recursively

$$p_i = r^{i-1} - \sum_{k=1}^{i-1} \frac{\langle r^{i-1}, p_k \rangle}{\langle p_k, p_k \rangle} p_k, \qquad i = 2, 3, \ldots m \tag{21}$$

where $r$ is the radial distance from the given point $\vec{x}(r = \sqrt{x^2 + y^2})$. Taking the linear system expressed by (11),

$$A(\vec{x}) a(\vec{x}) = B(\vec{x}) u \tag{22}$$

substituting the expressions for $\boldsymbol{A}$ and $\boldsymbol{B}$ (13), (14), (15), (16) and recalling the orthogonality conditions (19), the following linear system is obtained

$$\begin{bmatrix} \langle p_1, p_1 \rangle & \cdots & 0 \\ \vdots & \ddots & \vdots \\ 0 & \cdots & \langle p_m, p_m \rangle \end{bmatrix} \begin{bmatrix} a_1(\vec{x}) \\ \vdots \\ a_m(\vec{x}) \end{bmatrix} = \begin{bmatrix} \langle p_1, u \rangle \\ \vdots \\ \langle p_m, u \rangle \end{bmatrix}. \tag{23}$$

This system, when solved for $a$ gives

$$\begin{bmatrix} a_1(\vec{x}) \\ \vdots \\ a_m(\vec{x}) \end{bmatrix} = \begin{bmatrix} \frac{1}{\langle p_1, p_1 \rangle} & \cdots & 0 \\ \vdots & \ddots & \vdots \\ 0 & \cdots & \frac{1}{\langle p_m, p_m \rangle} \end{bmatrix} = \begin{bmatrix} \langle p_1, u \rangle \\ \vdots \\ \langle p_m, u \rangle \end{bmatrix}. \tag{24}$$

Calling this new matrix $\overline{A}(\vec{x})$ and as $(\langle p_1, u \rangle, \ldots, \langle p_m, u \rangle) = B(\vec{x})u$, we have for the coefficients $a$

$$a(\vec{x}) = \vec{A}(\vec{x})B(\vec{x})u \tag{25}$$

which is an expression analogous to (11), but requires no matrix inversion. Once the inner products are always positive and different from zero, $\overline{A}$ is always nonsingular, thus providing correct values for the coefficients $a$. (25) is then substituted back in (5), and a comparison with (4) makes explicit the expression for the shape functions

$$\Phi(\vec{x}) = [\phi_1(\vec{x}), \ldots, \phi_N(\vec{x})] = p^T(\vec{x})\vec{A}(\vec{x})B(\vec{x}). \tag{26}$$

## IV. Numerical Procedures

The problem at hand consists of numerically evaluating the integral (1), (2) or (3) in order to obtain the surface electric current $J_z$. Nodes are then spread along the perimeter of the cylinder cross section (Fig. 2). Expressing the surface current as a sum of shape functions built through the MLS or IMLS approximations there follows:

$$J_z(\vec{x}) = \sum_{i=1}^{N} \phi_i(\vec{x})\widehat{u}_i. \tag{27}$$

Enforcing the CFIE (3) at each observation point $\vec{x}_i$ and taking the shape function expansion for $J_z$, we get the following linear system in $u$

$$\sum_{j=1}^{N} K_{ij}^c \widehat{u}_j = f_i^c \tag{28}$$

$$K_{ij}^c = \alpha K_{ij}^e + (1+\alpha)\eta K_{ij}^m \tag{29}$$

$$f_i^c = \alpha f_i^e + (1+\alpha)\eta f_i^m \tag{30}$$

$$K_{ij}^e = \frac{\omega\mu}{4} \oint \phi_j(\vec{x}') H_0^{(2)}(kR) dl' \tag{31}$$

$$K_{ij}^m = \frac{1}{2}\phi_j(\vec{x}_i) + \frac{jk}{4} \oint \phi_j(\vec{x}') H_1^{(2)}(kR)[\widehat{n} \cdot \widehat{R}] dl' \tag{32}$$

$$f_i^e = E_z^i(\vec{x}_i) \tag{33}$$

$$f_i^m = \left\{ \widehat{n} \times \widehat{H}_i(\vec{x}_i) \right\} \cdot \widehat{z} \tag{34}$$

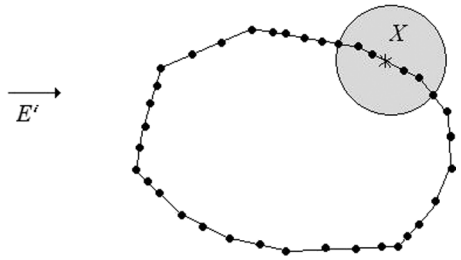


Fig. 2. Nodes are spread along the perimeter of a general-shaped conducting cylinder. Those nodes that influence a given point X are shown inside the shaded region.

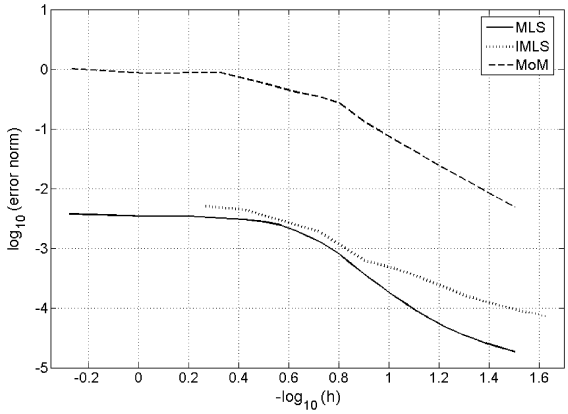


Fig. 3. Convergence of the error norm as a function of the discretization length $h$ (distance between two adjacent nodes) for MoM (unit pulse basis and delta testing functions), MLS, and IMLS approximations.

and $H_1^{(2)}$ is the first order Hankel function of the second type. In (32) and (34), the terms were obtained from (2) after some vector manipulation. Once the $\widehat{u}_i$ parameters are found, the surface current density at a given $\vec{x}$ can be determined by first finding the nodes that influence $\vec{x}$ and then applying (27). (If the EFIE is to be employed alone, $\alpha$ shall be set to 1; otherwise, if only the MFIE is desired, $\alpha$ shall be set to 0.)

## V. Results

In order to evaluate the convergence of the method, we first considered the scattering of a plane wave by a circular perfect electric conductor (PEC) cylinder. This problem possesses analytical solution, thus providing a means to study the precision of the numerical results (details can be seen in [2]). For a set of shape functions built through the MLS approximation, and employing a RMS norm

$$norm = \sqrt{\frac{1}{2\pi a} \oint \left[ J_{z_{Analytical}} - J_{z_{Numerical}} \right]^2 dl'} \tag{35}$$

($a$ is the radius of the cylinder, equal to 10 wavelengths) we have found out that the MLS with a linear basis works better than the MoM with pulse basis functions, according to Fig. 3. Solving the same problem for the circular cylinder but employing a new set of shape functions now built through IMLS, we can establish a comparison between both approximations and thus find out which of them works better (Fig. 3 again). The results seem to indicate that the scenario for IMLS is worse; its convergence

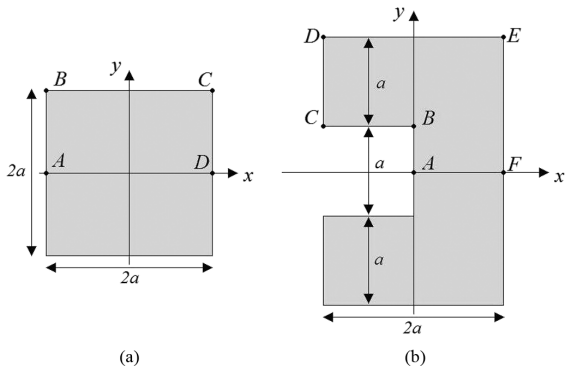


Fig. 4. Non-circular cross sections ($a = \lambda/2\pi$).

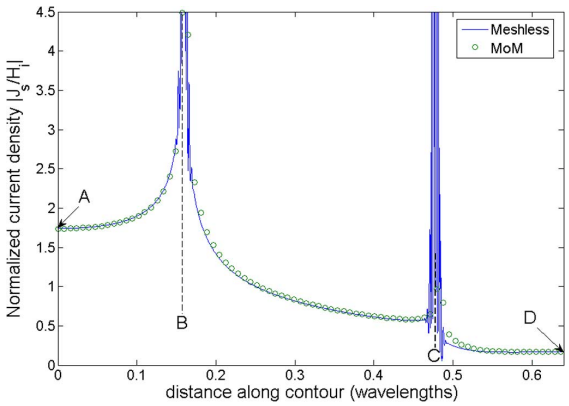


Fig. 5. Normalized current density amplitude ($J_z/H^i$) along the perimeter section ABCD of Fig. 4(a).

rate is smaller and its error is greater. But the MLS approximation does not work in every situation. For a scatterer whose cross section is a square, or a rectangle, for example, singular $\boldsymbol{A}$ matrices are obtained, thus leading to the impossibility of getting the shape functions. The reason is that for points lying in regions along the sides, *away from the corners*, the parameter that describes the contour line experiences variation only in one variable ($x$ only or $y$ only). For example, a given point $\vec{x}$ in the square upper side has a constant $y$-coordinate, $y = c$ (side BC in Fig. 4). So the basis becomes $p = [1, x, c]^T$. One sees that all $N$ nodes whose influence domains act upon $\vec{x}$ have the $y$-coordinate equal to $c$; then all third column elements of the $\boldsymbol{P}$-matrix (15) are equal to $c$ as well. Consequently, $\boldsymbol{P}$ has two constant columns. So, the product $\boldsymbol{A} = \boldsymbol{P^T W P}$ will have two linearly dependent columns. Hence, $\boldsymbol{A}$ is singular.

One way to solve that is to make the nodal influence domains as large as the side of the square, in order to make sure that inside this domain there will be points distributed along two adjacent sides. By doing this, both $x$ and $y$ will vary, $\boldsymbol{P}$ will no longer have two linearly dependent columns and $\boldsymbol{A}$ shall not be singular. But it revealed to be a bad approach: one sees that as the influence domains become larger, the local perspective of the method is destroyed. Besides that, the results are not so much accurate.

In order to verify the feasibility of the IMLS method, we applied it to two cross-sectional geometries that could be "patho-

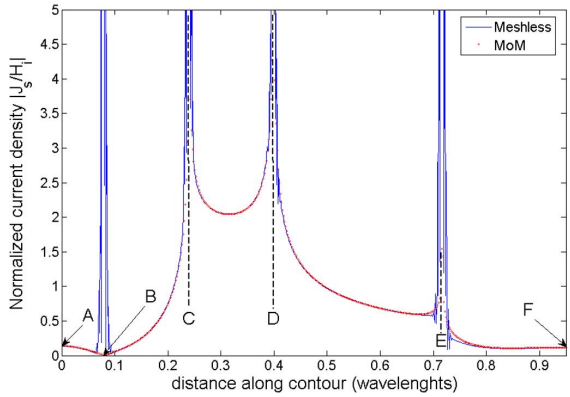


Fig. 6. Normalized current density amplitude ($J_z/H^i$) along the perimeter section ABCDEF of Fig. 4(b).

logical" to the eyes of the MLS method, i.e., scatterers with flat sides (Figs. 4–6). The parameter $a$ was set equal to $\lambda/2\pi$, where $\lambda$ is the wavelength. These problems illustrate the scattering of a $\mathrm{TM^z}$ plane wave of unit amplitude propagating in the direction $x(e^{-jkx})$.

The results of Figs. 5 and 6 show that the meshless approach via IMLS provides reasonable results when compared to MoM, as long as the points of interest lie far from the edges, where theoretically predicted singularities in the surface current density occur. We found that the IMLS shape functions go through strong peaks near the edges, thus providing very poor results there.

## VI. Conclusion

In this paper we extended to scatterers with non-circular cross sections the procedure developed in a previous work [2]. The IMLS approximation presents good results where the MLS cannot find a solution, i.e., along the flat sides of the scatterer. However, the IMLS solution exhibits strong peaks and oscillatory results near corners. Ways to avoid errors caused by abrupt discontinuities of the surface curvature (e.g., corners) will be the theme for a future work.

## Acknowledgment

This work was supported in part by the State of Minas Gerais Research Foundation-FAPEMIG, Brazil, under grant Pronex TEC 01075/09 and TEC-APQ-00852-08, and by CAPES, Brazil, under grant RH-TVD-254/2008.

## References

[1] A. Manzin and O. Bottauscio, "Element-free Galerkin method for the analysis of electromagnetic-wave scattering," *IEEE Trans. Magn.*, vol. 44, no. 6, pp. 1366–1369, 2008.

[2] W. L. Nicomedes, R. C. Mesquita, and F. J. S. Moreira, "An integral meshless-based approach in electromagnetic scattering," *COMPEL*, vol. 29, no. 6, 2010, to be published.

[3] G. R. Liu, *Mesh Free Methods: Moving Beyond the Finite Element Method*. Boca Raton, FL: CRC Press.

[4] M. Peng and Y. Cheng, "A boundary element-free method (BEFM) for two-dimensional potential problems," *Eng. Anal. With Boundary Elements*, vol. 33, no. 1, pp. 77–82, 2009.